Mesophyll conductance to CO2, assessed from online TDL-AS records of (CO2)-C-13 discrimination, displays small but significant short-term responses to CO2 and irradiance in Eucalyptus seedlings

Cyril C. Douthe, Erwin Dreyer, Daniel D. Epron, Charles R. Warren

HAL Id: hal-02644469
https://hal.inrae.fr/hal-02644469

Submitted on 28 May 2020

Journal of
Experimental
Botany
www.jxb.oxfordjournals.org

RESEARCH PAPER

Mesophyll conductance to CO_2, assessed from online TDL-AS records of $^{13}CO_2$ discrimination, displays small but significant short-term responses to CO_2 and irradiance in *Eucalyptus* seedlings

Cyril Douthe[1,2,3], Erwin Dreyer[1,2,*], Daniel Epron[1,2] and Charles R. Warren[3]

[1] INRA, Unité Mixte de Recherches 1147 'Ecologie et Ecophysiologie Forestières', F-54280 Champenoux, France

[2] Nancy Université, Unité Mixte de Recherches 1147 'Ecologie et Ecophysiologie Forestières', Faculté des Sciences, F-54500 Vandoeuvre, France

[3] University of Sydney, School of Biological Sciences, Heydon-Laurence Building, A08, The University of Sydney, NSW 2006, Australia

* To whom correspondence should be addressed. E-mail: dreyer@nancy.inra.fr

Abstract

Mesophyll conductance (g_m) is now recognized as an important limiting process for photosynthesis, as it results in a significant decrease of CO_2 diffusion from substomatal cavities where water evaporation occurs, to chloroplast stroma. Over the past decade, an increasing number of studies proposed that g_m can vary in the short term (e.g. minutes), but these variations are still controversial, especially those potentially induced by changing CO_2 and irradiance. In this study, g_m data estimated with online ^{13}C discrimination recorded with a tunable diode laser absorption spectrometer (TDL-AS) during leaf gas exchange measurements, and based on the single point method, are presented. The data were obtained with three *Eucalyptus* species. A 50% decrease in g_m was observed when the CO_2 mole fraction was increased from 300 μmol mol^{-1} to 900 μmol mol^{-1}, and a 60% increase when irradiance was increased from 200 μmol mol^{-1} to 1100 μmol mol^{-1} photosynthetic photon flux density (PPFD). The relative contribution of respiration and photorespiration to overall ^{13}C discrimination was also estimated. Not taking this contribution into account may lead to a 50% underestimation of g_m but had little effect on the CO_2- and irradiance-induced changes. In conclusion, (i) the observed responses of g_m to CO_2 and irradiance were not artefactual; (ii) the respiratory term is important to assess absolute values of g_m but has no impact on the responses to CO_2 and PPFD; and (iii) increasing irradiance and reducing the CO_2 mole fraction results in rapid increases in g_m in *Eucalyptus* seedlings.

Key words: *Eucalyptus globulus*, *Eucalyptus saligna*, *Eucalyptus sieberii*, photosynthesis, stomatal conductance, tunable diode laser absorption spectrometry.

Introduction

During photosynthesis, CO_2 diffuses from the atmosphere (at a mole fraction C_a) to the sites of carboxylation (C_c) inside the chloroplasts (Gaastra, 1959; Farquhar *et al.*, 1980). CO_2 crosses the leaf boundary layer and traverses stomatal pores into the substomatal cavity. CO_2 then diffuses through the gas phase between mesophyll cells before reaching cell walls, where it is solubilized. In the liquid phase, CO_2 crosses the plasma membrane, the cytosol, and finally the chloroplast membranes to reach the sites of carboxylation in the chloroplast stroma. Most of the carboxylation is by RubisCO (ribulose-1,5-bisphosphate carboxylase/oxygenase), while a small fraction (estimated at 5%) is by phospho*enol*pyruvate carboxylase (PEPc) in the cytosol. The mesophyll conductance to CO_2 (g_m) represents

the conductance from the substomatal cavities at a mole fraction C_i, to the sites of carboxylation, and includes gas and liquid phase transfer.

In early leaf photosynthesis models, g_m was considered to be infinite. This was an explicit assumption in the original formulation of Farquhar's model of C_3 photosynthesis. However, many subsequent studies showed that there was a difference between C_i and C_c, suggesting that g_m might be finite (Evans *et al.*, 1986; Lloyd *et al.*, 1992) and that it affects estimation and interpretation of photoynthetic parameters such as the maximal carboxylation activity of RubisCO (V_{cmax}) or the maximal light-driven electron flux (J_{max}) (Epron *et al.*, 1995; Niinemets *et al.*, 2009a). g_m can limit the rate of photosynthesis by 25–30% (Epron *et al.*, 1995) and this limitation may be as large as the one due to stomatal conductance (Warren and Adams, 2006; Flexas *et al.*, 2007c). The range of g_m variation among species is similar to that of stomatal conductance, from 0.005 mol m^{-2} s^{-1} up to 0.5 mol m^{-2} s^{-1} (see the reviews by Evans and Von Caemmerer, 1996; Flexas *et al.*, 2008), with high g_m occurring in herbaceous annuals and lower values in evergreen gymnosperms. g_m is apparently influenced by leaf traits such as thickness, tissue density (and therefore leaf dry mass per unit area, LMA; for meta analyses, see Flexas *et al.*, 2008; Niinemets *et al.*, 2009b), cell wall thickness, or the proportion of gaseous versus liquid mesophyll phases (Piel *et al.*, 2002; Terashima *et al.*, 2006; Evans *et al.*, 2009). Such morphological leaf properties would confer stable g_m in the short term (e.g. a few days).

Since the early 1990s, g_m was shown to be affected by environmental factors. At first, changes were thought to be rather long-term changes such as, for instance, the decline induced by leaf ageing (Scartazza *et al.*, 1998), by a gradual drought stress (Cornic *et al.*, 1989; Roupsard *et al.*, 1996; Warren, 2008b), or by salinity (Bongi and Loreto, 1989). More recently, short-term changes were shown to occur in response to temperature (Bernacchi *et al.*, 2002; Pons and Welschen, 2003; Warren and Dreyer, 2006; Warren, 2008a). Similarly rapid responses of g_m (at the minutes scale) were reported to occur under varying CO_2 mole fractions. A review by Flexas *et al.* (2008) reported that g_m decreases with increasing CO_2 (data from Harley *et al.*, 1992; During, 2003; Flexas *et al.*, 2007b). This pattern was also observed by Hassiotou *et al.* (2009) among seven *Banksia* species, by Vrabl *et al.* (2009) in *Helianthus annus*, and by Bunce (2010) in *Glycine max* and *Phaseolus vulgaris*. Tazoe *et al.* (2011) recently observed the same decreasing pattern among three species with contrasting photosynthetic capacities. Only a few studies have tested the rapid response of g_m to irradiance. Flexas *et al.* (2008) reported an increase of g_m with increasing irradiance (data from Gorton *et al.*, 2003; Flexas *et al.*, 2007b).

Nevertheless, there is still no consensus about the reality of such rapid responses of g_m to CO_2 and irradiance. Several studies reported g_m to be stable in response to changes in CO_2 (Von Caemmerer and Evans, 1991; Loreto *et al.*, 1992; Tazoe *et al.*, 2009) and irradiance (Tazoe *et al.*, 2009; Yamori *et al.*, 2010). Some of the discrepancy may be due to measurement accuracy and/or artefacts. This can be true with the two main methods used to estimate g_m: the fluorescence/gas exchange technique (Loreto *et al.*, 1992) and the isotopic discrimination method (Pons *et al.*, 2009). One of the complications with the isotopic method, which is used here, is that the contribution of ^{13}C discrimination during respiration and photorespiration needs to be taken into account (see the model description below). Some studies have ignored discrimination during respiration and photorespiration (Flexas *et al.*, 2007b, c; Vrabl *et al.*, 2009), or approximated respiration in the light by that in the dark (Tazoe *et al.*, 2009, 2011). The fractionation factors associated with respiration and photorespiration can be taken into consideration using recent estimates (Lanigan *et al.*, 2008). An alternative approach is to limit the impact of fractionation during photorespiration by using low O_2 in the measurement atmosphere (Tazoe *et al.*, 2009).

To date, there is no consensus regarding whether g_m responds rapidly to irradiance and the CO_2 mole fraction, despite the importance of this for interpreting responses of photosynthesis to environmental variables. The aim of this research was to assess whether short-term variations of g_m occur in response to changes in irradiance and the CO_2 mole fraction. Rapid response of g_m was assessed by recording online $^{13}CO_2$ discrimination during photosynthesis with a custom-built photosynthesis chamber adapted to a LI-COR 6400, and coupled to a TDL-AS (or tunable diode laser absorption spectrometer). To examine the ubiquity of responses, three species of *Eucalyptus* with differing rates of photosynthesis were used, and the respiratory term of online ^{13}C discrimination was taken into consideration to reinforce the findings. Measurements were carried out on species with contrasting photosynthetic capacity to check whether g_m variability is species dependent and how g_m is related to A and g_s within and among species.

Materials and methods

Plant material

Three species in the genus *Eucalyptus* were used: *E. globulus* Labill., *E. saligna* Sm., and *E. sieberi* L. A. S. Johnson. Plants were grown for 4 months in a naturally illuminated greenhouse at an average daily temperature of 25 °C in 8.0 l pots filled with compost-based substrate. They were watered with automatic drip irrigation. At the time of the experiment they were ~60 cm high.

Gas exchange measurements

The response of the net CO_2 assimilation rate (A, µmol m^{-2} s^{-1}) to variations in substomatal CO_2 mole fraction (C_i) and photosynthetic photon flux density (PPFD, µmol m^{-2} s^{-1}) was measured in each of four replicate plants of the three species, for each treatment (e.g. 2 treatments×3 species×4 replicates=24 plants). All measurements were made on the youngest fully expanded leaves. Plants were transferred from the greenhouse to the laboratory at 25 °C. To assess photosynthesis and discrimination against $^{13}CO_2$ simultaneously, a LI-6400 portable gas exchange system (LI-COR, Lincoln, NE, USA) equipped with a custom-built chamber of 18 cm^2 and coupled to a TDL-AS (TGA100A, Campbell Scientific, Logan, UT, USA) was used.

Before measurements, leaves were exposed to 1000 µmol m^{-2} s^{-1} PPFD and 400 µmol CO_2 mol^{-1} for 30 min to induce photosynthesis and stomatal opening. CO_2 responses of photosynthesis were measured under a constant PPFD of 1000 µmol m^{-2} s^{-1} while the CO_2 mole fraction for the reference gas (C_e) was sequentially set at 300, 500, 700, and 900 µmol mol^{-1}. The PPFD responses at 200, 500, 800, and 1100 µmol m^{-2} s^{-1} were measured under a constant CO_2 mole fraction of 400 µmol mol^{-1}. During each step of the CO_2 or PPFD responses, at least 20 min was allowed for A and g_s to reach a steady state, and three individual points separated by 180 s were recorded. Each set of three individual data points was averaged to characterize the response at one step in the response curve. The standard error of the three individual points was used to assess the analytical variability.

Air flow into the chamber was set at 400 µmol s^{-1}, and leaf temperature at 25 °C. Irradiance was provided by a LI-COR RGB light source (6400-18, LI-COR-0128), which covered the entire chamber surface. A subsample of air from the sample and reference gas lines of the LI-6400 was diverted to the TDL-AS. The TDL-AS measured sequentially gas from two calibration tanks, the LI-6400 reference gas, and finally the LI-6400 sample gas. Each intake was measured for 45 s, with the first 15 s ignored to minimize carryover and enable stabilization between intakes. The total time for a sequence of measurements was therefore 180 s.

The TDL-AS gas was connected through a 'T' tubing to the reference tube of the LI-6400 between the console and the IRGA. In the same way, the TDL-AS intake of sample gas was connected in between the LI-6400 chamber exhaust. The TDL-AS was set to continuously withdraw 150 ml min^{-1} (~102 µmol s^{-1}) from each of the sample and reference fluxes of the LI-6400. This withdrawal of air was much smaller than the flow through the LI-6400 chamber, which means that the TDL-AS could sample air from the LI-6400 while maintaining a positive pressure in the LI-6400 chamber. The existence of a positive pressure inside the LI-6400 chamber was checked through the curvature of the propafilm covering the top of the chamber. TDL-AS data were matched with LI-6400 data by taking into account the time lag of 37 s that was recorded between the chamber and the TDL-AS. The TDL-AS data were only used to record the isotopic composition of the reference and sample gas, while all photosynthesis parameters were estimated from the LI-6400 data.

Isotopic measurements and system testing

Discrimination by a leaf was assessed by measuring the isotopic composition in reference ($\delta^{13}C_e$, ‰) and sample gas ($\delta^{13}C_o$, ‰). The isotopic composition ($\delta^{13}C$) was expressed as:

$$\delta = \left(\frac{R_S}{R_{VPDB}} - 1 \right) \times 1000$$

where R_s is the isotopic ratio ($R = ^{13}CO_2/^{12}CO_2$) of the sample and R_{VPDB} is the isotopic ratio of Vienna Pee Dee Belemnite (VPDB, 0.0112372).

The TDL-AS was calibrated with two tanks (T1 and T2) with CO_2 concentrations of 419±10 µmol mol^{-1} and 290±7 µmol mol^{-1} [mean ± the confidence interval (CI)], respectively, given by the provider and checked with a recently factory-calibrated LI-8100 IRGA (LI-COR). The isotopic composition of the each tank was measured by sampling air into 12 ml exetainers (Labco Limited, Buckinghamshire, UK) and analysed via the gas-bench inlet of an IRMS (Delta S, Finningan, Bremen, Germany) at INRA Nancy ($n=10$ exetainers per tank). For T1 and T2, $\delta^{13}C$ was –36.6±0.08‰ and –36.9±0.2‰ [mean ± standard deviation (Sd), $n=10$], respectively. Absolute values of $^{12}CO_2$ and $^{13}CO_2$ were, respectively, 414.51 µmol mol^{-1} and 4.487 µmol mol^{-1} for T1 and 286.89 µmol mol^{-1} and 3.104 µmol mol^{-1} for T2, considering the CO_2 mole fraction indicated by the provider took into consideration both isotopologues. A linear interpolation was

used between these two points for each isotopologue. For further calibration, a range of CO_2 mole fractions of 200, 300, 500, 700, 1000, 1500, and 2000 µmol mol^{-1} was generated using the CO_2 injector of the LI-6400 fed with the same CO_2 cartridge during the whole test. CO_2 mole fractions above the calibration range led to a small deviation of +2.5‰. A second order polynom was fitted to describe the deviation of apparent $\delta^{13}C$ from reference values measured at $C_e=300$ µmol mol^{-1} (because this is within the calibration range) along the extended CO_2 range ($\delta^{13}C=0.000007[CO_2]^2-0.0035[CO_2]-5.2922$; $R^2=0.92$, $n=140$). All TDL-AS values were corrected and a stable $\delta^{13}C$ signal was obtained along the extended CO_2 mole fraction range.

The noise of the system was assessed by observing the Sd of $\delta^{13}C$ values within each CO_2 step. An average Sd of 0.16 ‰ was observed for $\delta^{13}C$ ($n=21$). These values were used for the computation of the standard deviation of the observed discrimination by the leaf (Sd$_{\Delta obs}$, see below).

Finally the empty photosynthesis chamber was used to test the absence of a $\delta^{13}C$ difference between the inlet and outlet that might be caused by leaks and/or CO_2 adsorption/desorption processes. It was observed that the $\delta^{13}C_e–\delta^{13}C_o$ difference was stable along the CO_2 mole fraction range used during the test, and it was confirmed that the empty chamber did not affect the isotopic composition of the air (i.e. leaks and CO_2 adsorption/desorption processes were negligible). The observed $\delta^{13}C_e–\delta^{13}C_o$ difference was much smaller than the $\delta^{13}C$ difference recorded during actual measurements (Fig. 1), although under specific conditions (low photosynthesis) the two could overlap. A data filtering procedure was therefore implemented (see below).
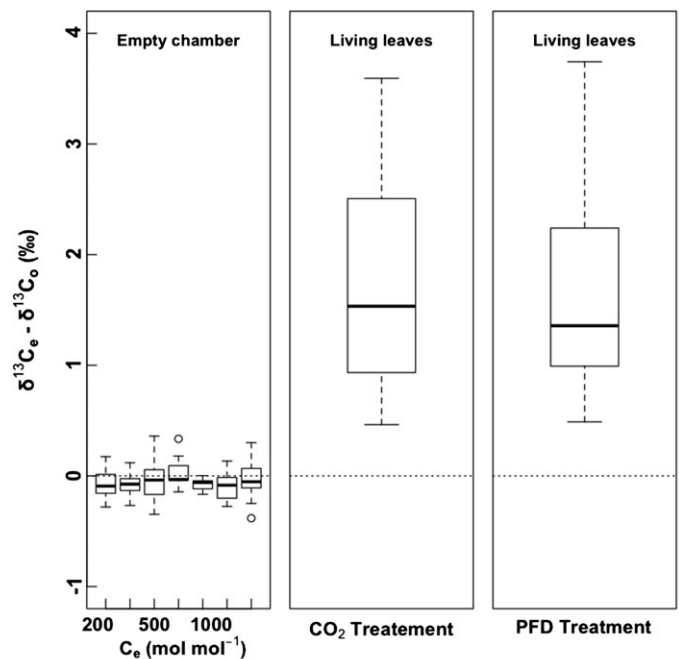
Fig. 1. Boxplots of the difference in $\delta^{13}C$ between the outlet and inlet of the 18 cm^2 chamber for (i) an empty chamber with inlet air CO_2 varying from 200 µmol mol^{-1} to 1000 µmol mol^{-1} ($n=10$); (ii) the whole set of measurements under varying CO_2 concentrations (300 µmol mol^{-1} to 900 µmol mol^{-1}), $n=40$; and (iii) the whole set of measurements under varying PPFD (from 200 µmol m^{-2} s^{-1} up to 1100 µmol m^{-2} s^{-1}), $n=40$. The middle line represents the median, the upper and lower box limit the 75% and 25% quartiles, respectively, and whiskers represent the extreme value.

Model description

The observed discrimination (Δ_{obs}) is usually calculated following Evans *et al.* (1986):

$$\Delta_{obs} = \frac{\xi\left(\delta^{13}C_o - \delta^{13}C_e\right)}{1000 + \delta^{13}C_o - \xi\left(\delta^{13}C_o - \delta^{13}C_e\right)} \quad (1)$$

where:

$$\xi = \frac{C_e}{C_e - C_o} \quad (2)$$

ξ is the ratio of CO_2 entering the chamber over the CO_2 drawdown induced by the leaf.

Δ is the result of discrimination by diffusion processes during CO_2 movement from the atmosphere to the chloroplast, and biochemical fractionation during carboxylation processes. Each fractionation step is characterized by a fractionation factor (due to diffusion or biochemistry) weighted by the gradient of concentration. In the complete form, Δ is predicted by (Evans *et al.*, 1986):

$$\Delta = a_b \frac{C_a - C_s}{C_a} + a \frac{C_s - C_i}{C_a} + \left(e_s + a_i\right)\frac{C_i - C_c}{C_a} + b\frac{C_c}{C_a}$$
$$- \frac{\frac{eR_d}{k} + f\Gamma*}{C_a} \quad (3)$$

where:

- a_b is the fractionation during CO_2 diffusion in the boundary layer (2.9‰, Evans *et al.*, 1986);
- a is the fractionation during CO_2 diffusion in air through stomata into the leaf (4.4‰, O'Leary, 1981);
- e_s is the fractionation occurring when CO_2 is dissolved in the cell solution (1.1‰ at 25 °C, O'Leary, 1981);
- a_i is the fractionation during CO_2 diffusion in the liquid phase (0.7‰, O'Leary, 1981);
- b is the discrimination during carboxylation, and is dependent on fractionation by both RubisCO (b_3=30‰) and PEPc (b_4= –5.7‰),

b is computed as:

$$b = (1 - \beta)b_3 - \beta b_4 \quad (4)$$

where β (between 0.05 and 0.1) is the relative amount of carbon fixed by PEPc (Farquhar and Richards, 1984). In the present experiment a value of b=28‰ was used; that is, a β value of 0.055.
- f denotes overall discrimination during photorespiration. The value of f was set at 11‰, according to the theoretical approach of Tcherkez (2006), which was confirmed later by Lanigan *et al.* (2008);
- e denotes overall fractionation during day respiration relative to photosynthetic products (R_d), and can vary between –10‰ and +10‰ (Ghashghaie *et al.*, 2003). e was set at 1‰ before correction following Wingate *et al.* (2007);
- k is the carboxylation efficiency computed as (Farquhar *et al.*, 1982);

$$k = (A + R_d)/(C_i - \Gamma*) \quad (5)$$

- $\Gamma*$ is the CO_2 compensation point in the absence of day respiration (Brooks and Farquhar, 1985).

The estimation of g_m is based on the difference between the observed discrimination by the leaf (Δ_{obs}) and the discrimination predicted from the simplified form of the model (Δ_i) in which decarboxylation terms are ignored and g_m is considered to be infinite:

$$\Delta_i = a + \left(b - a\right)\frac{C_i}{C_a} \quad (6)$$

With this 'single point method' first developed by Lloyd *et al.* (1992) and recently described by Pons *et al.* (2009), g_m can be estimated from a single value of Δ_{obs}:

$$g_m = \frac{(b - e_s - a_i)A/C_a}{\left(\Delta_i - \Delta_{obs}\right) - \frac{eR_d/k + f\Gamma*}{C_a}} \quad (7)$$

Model parameters

R_d and $\Gamma*$ were estimated with the 'Laisk method' (Viil *et al.*, 1977) for the three species (i.e. from the intersection of three A–C_i curves recorded at PPFDs of 100, 50, and 25 µmol photon m^{-2} s^{-1} and C_e of 125, 100, and 50 µmol mol^{-1}). The 'Laisk method' provides C_i* or the 'apparent' CO_2 compensation point in the absence of day respiration (Von Caemmerer *et al.*, 1994), and was used as a proxy of $\Gamma*$. Because these measurements are sensitive to errors due to CO_2 leak diffusion (low A and low C_a compared with the atmosphere), the potential CO_2 leaks due to diffusion though chamber gaskets were estimated (Flexas *et al.*, 2007a; Rodeghiero *et al.*, 2007). A diffusion coefficient of the gaskets was computed with the procedure provided in the user manual of LI-COR, and a value of 0.938 µmol s^{-1} was found (while it usually is 0.46 for smaller 6 cm^2 chambers). This correction was incorporated into all gas exchange computations used for $\Gamma*$ and R_d estimations. The computed values of $\Gamma*$ did not differ between species, so the mean ($\Gamma*$=38.7±0.51 µmol mol^{-1}, n=13) was used as a common value for the three species. For *E. globulus*, *E. saligna*, and *E. sieberi*, R_d was 0.41±0.09, 0.31±0.09, and 0.68±0.07 µmol m^{-2} s^{-1}, respectively.

As the isotopic signature of the reference gas provided by cartridges differed from that used by the leaves for earlier photosynthesis, e was replaced by e'=e+$\delta^{13}C_{tank}$–$\delta^{13}C_{atmosphere}$ (Wingate *et al.*, 2007). $\delta^{13}C$ in the cartridge was measured with the TDL-AS at the chamber inlet. In the present case, the LI-6400 was fed with compressed CO_2 cartridges with $\delta^{13}C_{tank}$ varying between –1‰ and –4‰ except for two cartridges with $\delta^{13}C_{tank}$= –19‰. e' therefore varied between +4‰ and +6‰, except for two plants where it was –11‰.

C_c, the CO_2 concentration at the site of carboxylation, was calculated from Fick's Law as:

$$C_c = C_i - \frac{A}{g_m} \quad (8)$$

Finally, the total leaf conductance to CO_2 was calculated following Ball (1988), assuming resistances in series as:

$$g_t = \frac{1}{\frac{1}{g_{sc}} + \frac{1}{g_m}} \quad (9)$$

where the stomatal conductance to CO_2 is g_{sc}=g_{sw}/1.6.

Propagation of uncertainty from measurement to Δ calculation and data filtering

The uncertainty (standard deviation) of Δ_{obs} due to the finite precision of $\delta^{13}C$ measurements was estimated. This was achieved by propagating uncertainty (standard deviations) of $\delta^{13}C_e$ and $\delta^{13}C_o$ through the equations estimating Δ_{obs} (see Appendix for details):

$$Sd_{\Delta obs} = \left(\frac{\xi \sqrt{Sd_{\delta 13Ce}^2 + Sd_{\delta 13Co}^2}}{\xi \left(\delta^{13}C_o - \delta^{13}C_e \right)} + \frac{1 + \sqrt{Sd_{\delta 13Co}^2} - \xi \sqrt{Sd_{\delta 13Ce}^2 + Sd_{\delta 13Co}^2}}{1 + \delta^{13}C_o - \xi \left(\delta^{13}C_o - \delta^{13}C_e \right)} \right) \Delta_{obs} \quad (10)$$

The propagated uncertainty in Δ_{obs} (i.e. $Sd_{\Delta obs}$) was used as the basis for a filter to remove unreliable estimates of Δ_{obs}. Computation of g_m is based on the difference between Δ_i and Δ_{obs} (i.e. Δ_i–Δ_{obs}), thus it was reasoned that g_m estimates would be unreliable if the difference Δ_i–Δ_{obs} was smaller than $Sd_{\Delta obs}$. Consequently all values where $\Delta_{obs}+Sd_{\Delta obs} > \Delta_i$ were rejected. This filter was applied to the individual points in the data set, rejecting 33 among 238 points.

Statistical analyses

All statistical analyses were performed with R (R Development Core Team 2010, http://www.R-project.org). Mixed-effect linear models were run to assess species and treatment effects on A, g_s, g_m, Δ_i–Δ, C_c, and the C_i–C_c drawdown, as shown in Table 1. For the CO_2 treatment, 'species' (as a factor) and 'C_i' (as a covariate) were incorporated into the model as fixed effects, and 'individual within species' as a random effect. For variations of C_c and the C_i–C_c drawdown, C_a was used as covariate. For PPFD treatment, species and PPFD were set as factors. Normality and heteroscedasticity were graphically checked with QQ-plots. In the case of heteroscedastic data, the mean was weighted as a function of the variance. In the case of non-normal distribution, variables were log-transformed. The species×treatment interaction was tested for each procedure, and was removed from the model when not significant. In the absence of interaction, comparison of the intercepts was performed to assess differences between species. In the case of interaction, slope comparisons were performed to test if species responses differed from each other. Significance was accepted at $P < 0.05$. Mean least squares regression was used to assess the correlation between variables (R^2 and P-value).

Results

Variation of g_m under changing C_e

The CO_2 mole fraction was changed in the air entering the chamber in three steps from 300 µmol mol^{-1} to 900 µmol mol^{-1}, inducing a range of C_i from 185 µmol mol^{-1} to 745 µmol mol^{-1}. Net CO_2 assimilation rate (A) was positively related to C_i and varied between 3 µmol mol^{-2} s^{-1} and 18 µmol mol^{-2} s^{-1}, while stomatal conductance to water vapour (g_s) was negatively related to C_i and varied between 0.02 mol m^{-2} s^{-1} and 0.8 mol m^{-2} s^{-1} (Fig. 2). *Eucalyptus sieberi* had significantly higher A and g_s than *E. globulus* and *E. saligna* (*t*-test $P < 0.05$, Fig. 2).

The difference between $\delta^{13}C_e$ and $\delta^{13}C_o$ decreased with increasing C_i (data not shown). Among all species, Δ_{obs} varied between 12‰ and 22‰ and was positively correlated to C_i/C_a ($R^2 = 0.79$, $P < 0.001$, data not shown). The difference between Δ calculated with infinite g_m and no respiratory term (simple model) and observed Δ (Δ_i–Δ_{obs}) varied between 3‰ and 7‰ but showed no clear trend with C_i (Fig. 2, Table 1).

g_m computed by taking into account the respiratory component of discrimination varied from 0.025 mol m^{-2} s^{-1} to 0.55 mol m^{-2} s^{-1} (Fig. 2). g_m was larger in *E. sieberi* than in the other two species (*t*-test, $P < 0.05$). g_m was affected by C_i (Table 1), and decreased when C_i increased. Post-hoc tests revealed that *E. globulus* and *E. saligna* displayed g_m–C_i slopes significantly different from zero. In *E. sieberi*, three individuals out of four showed a clear negative pattern when C_i increased, but not the fourth. The relationship between g_m and g_s was significant among all species ($R^2 = 0.54$, $P < 0.001$), and within *E. globulus* and *E. saligna* when treated separately (data not shown).

C_c and the C_i–C_c drawdown were, as expected, severely affected by C_a (Table 1). The C_i–C_c drawdown was ∼50 µmol mol^{-1} at $C_a = 200$ µmol mol^{-1} and increased up to 200 µmol mol^{-1} at $C_a = 900$ µmol mol^{-1} (Fig. 3). When tested individually, all slopes of the responses of C_c and C_i–C_c to C_i were different from zero.

Variation of g_m with changing irradiance

A and g_s increased significantly with irradiance (Table 1). A and g_s were larger in *E. sieberi* than in the two other species (see Fig. 4, *t*-test $P < 0.05$). In each species, g_s increased significantly from 200 µmol m^{-2} s^{-1} to 500 µmol m^{-2} s^{-1} PPFD, and then stabilized (Fig. 4). A and g_s were positively correlated, for all species taken together (Fig. 5C, $R^2 = 0.76$, $P < 0.001$). Across the range of irradiance, Δ_{obs} varied between 11‰ and 20‰ and was positively correlated with C_i/C_a ($R^2 = 0.74$, $P < 0.001$, data not shown). Δ_i–Δ_{obs} varied between 3‰ and 9‰ but was not affected by irradiance or by species (Table 1, Fig. 4).

Table 1. Mixed effects model for A, g_s, g_m, and Δ_i–Δ

Species, C_a and C_i, or PPFD effects were incorporated into the model as fixed effects, and individual plant as a random effect. In the case of heteroscedastic data the mean was weighted as a function of the variance. For C_i and C_a, the degree of freedom (df) was 1, for PPFD df=3, and for species df=2. Significant values ($P < 0.05$) are shown in bold.

|		C_i				C_a		PPFD					
		A	**g_s**	**g_m**	**Δ_i–Δ**	**C_c**	**C_i–C_c**	**A**	**g_s**	**g_m**	**Δ_i–Δ**	**C_c**	**C_i–C_c**
Variable	*F*	**168.11**	**38.82**	**18.67**	3.70	**165.01**	**102.90**	**86.01**	**34.23**	**6.41**	NS	NS	NS
	P	**<0.001**	**<0.001**	**<0.001**	(0.06)	**<0.001**	**<0.001**	**0.001**	**<0.001**	**0.002**	NS	NS	NS
Species	*F*	**13.31**	**26.33**	**10.11**	**6.36**	**4.64**	**7.65**	**14.65**	(2.91)	NS	NS	NS	NS
	P	**0.002**	**<0.001**	**0.006**	**0.02**	**0.045**	**0.013**	**<0.01**	(0.10)	NS	NS	NS	NS
Interaction	*F*	3.05	NS	**3.44**	NS	**5.84**	**3.72**	**14.88**	**4.55**	NS	NS	NS	NS
	P	(0.06)	NS	**0.047**	NS	**0.008**	**0.038**	**<0.001**	**0.002**	NS	NS	NS	NS
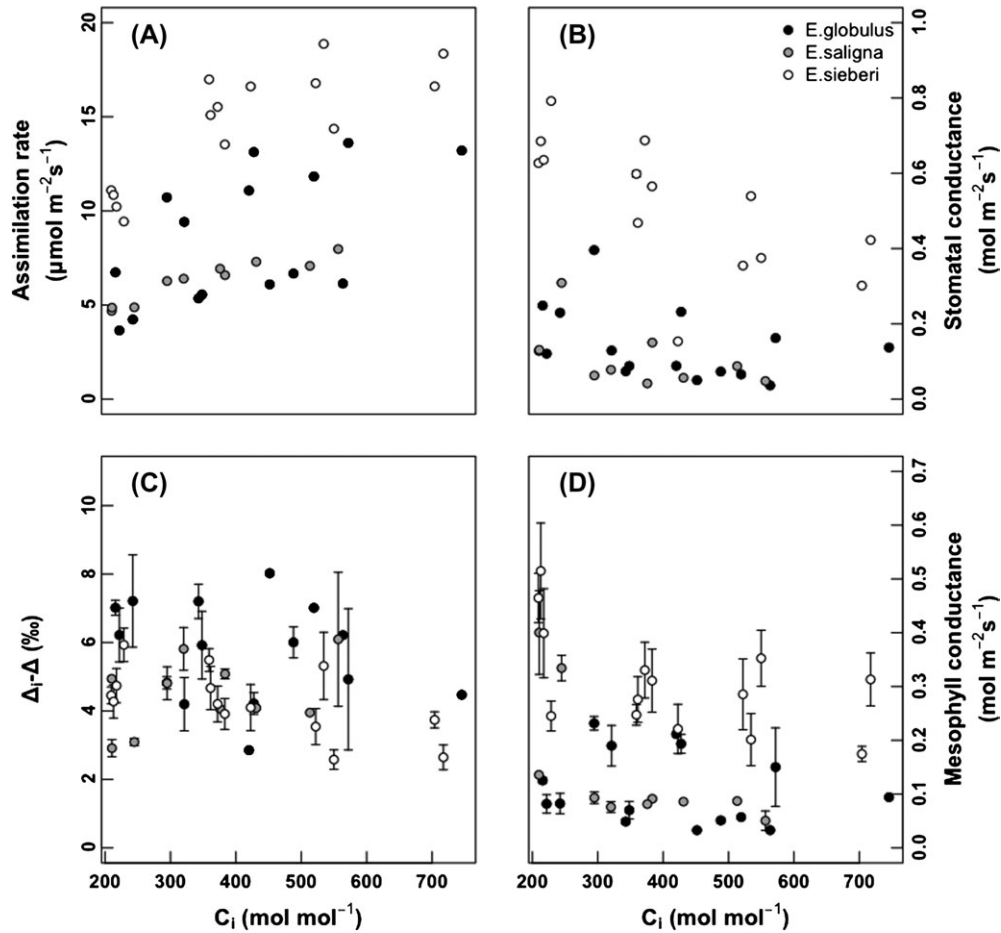
Fig. 2. Relationships between the CO_2 mole fraction in the substomatal cavities (C_i) and (A) net CO_2 assimilation rate (A). (B) Stomatal conductance to water vapour (g_s). (C) Difference between predicted and measured isotopic discrimination ($\Delta_i-\Delta$). (D) Mesophyll conductance (g_m). *Eucalyptus globulus* is in black, *E. saligna* in grey, and *E. sieberi* in white. The SE is provided by the average of three measurements taken at 180 s intervals. Measurements were made at four levels of C_e on four plants per species, and were filtered against noisy values of $\delta^{13}C_e-\delta^{13}C_o$.
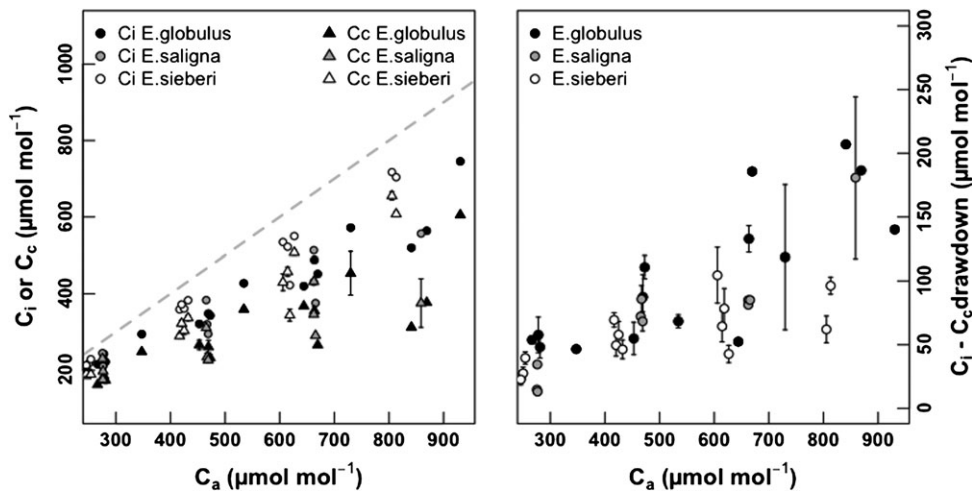

Fig. 3. Left: CO_2 mole fraction in the substomatal cavities (C_i, disks) and at carboxylation sites (C_c, triangles) as a function of C_a. The dashed grey line is the 1:1 relationship. Right: C_i–C_c drawdown as a function of C_a. Each point represents the mean of 1–3 analytical measurements ±SE, with *E. globulus* in black, *E. saligna* in grey, and *E. sieberi* in white.

g_m varied between 0.04 mol mol^{-2} s^{-1} and 0.6 mol mol^{-2} s^{-1}, and was positively related to PPFD. As for g_s, the response consisted of a significant increase between 200 µmol m^{-2} s^{-1} and 500 µmol m^{-2} s^{-1} PPFD with
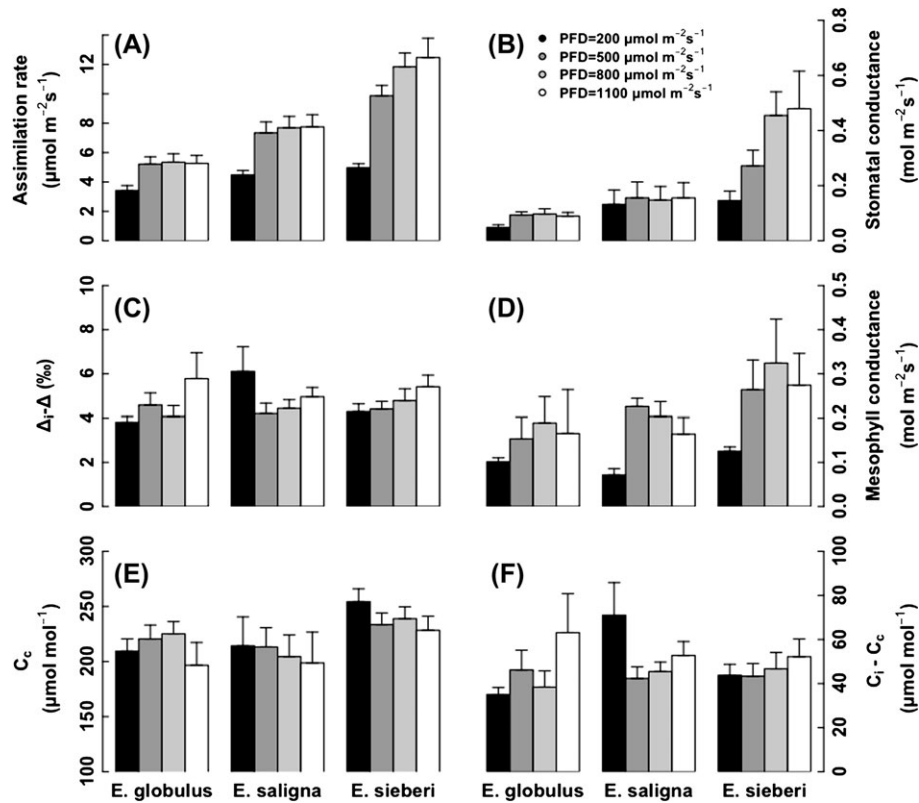
Fig. 4. (A) Net CO_2 assimilation rate (A). (B) Stomatal conductance to water vapour (g_s). (C) Difference between predicted and measured isotopic discrimination ($\Delta_i-\Delta$). (D) Mesophyll conductance (g_m). (E) CO_2 mole fraction at carboxylation sites (C_c). (D) The C_i–C_c drawdown at four different levels of PPFD. Means ±SE ($n=2$–4 replicate plants), with *E. globulus* in black, *E. saligna* in grey, and *E. sieberi* in white.
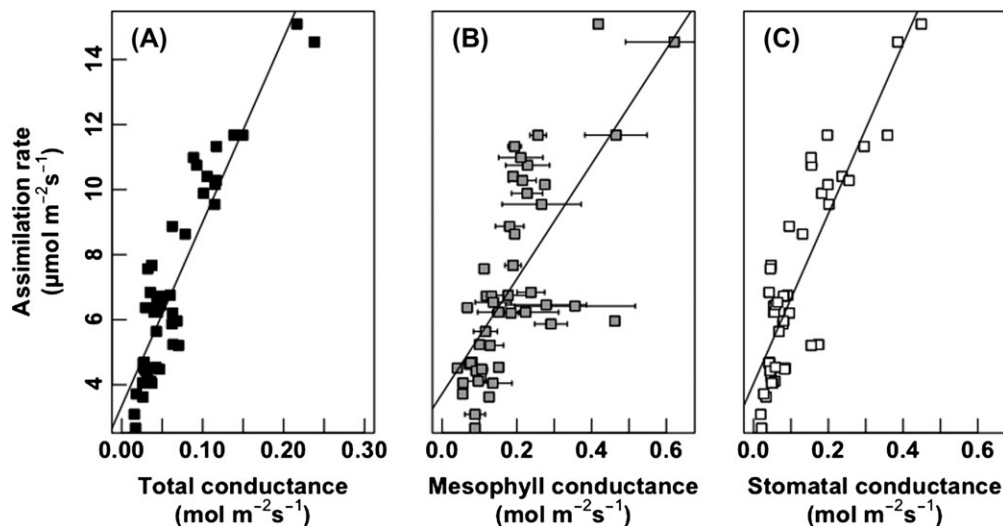
Fig. 5. Relationships between net CO_2 assimilation rate (A) and (A) total leaf conductance to CO_2 (g_t, black squares), (B) mesophyll conductance to CO_2 (g_m, grey squares), and (C) stomatal conductance to CO_2 (g_{sc}, white squares) under varying PPFD.

a stabilization above this threshold. g_m was positively correlated with g_s ($R^2=0.36$, $P<0.001$, data not shown) and A ($R^2=0.49$, $P<0.001$, Fig. 5B), among all species. Significant A–g_m and g_m–g_s relationships within each species were also detected (except for g_s–g_m in *E. saligna*).

Total leaf conductance to CO_2 (g_t) was strongly correlated to A ($R^2=0.83$, $P<0.001$) as shown in Fig. 5A. Over the full set of irradiance values, C_c varied between 200 µmol mol^{-1} and 260 µmol mol^{-1}, and the C_i–C_c drawdown between 40 µmol mol^{-1} and 60 µmol mol^{-1}. None of these

parameters displayed any variation with irradiance (Table 1), or with species.

Discussion

This study provides support to recent evidence that g_m varies rapidly (within minutes) in response to environmental conditions. The rapid responses were observed under two different sources of variation: CO_2 mole fraction and irradiance. In seedlings of three *Eucalyptus* species a modest but significant decrease of g_m with increasing CO_2 mole fraction, and a significant increase with irradiance, was found. The effect was visible in the three species irrespective of the photosynthetic capacity.

Importance of the respiratory and photorespiratory terms in the estimation of g$_m$

The isotopic method estimates g_m from the $^{13}CO_2$ discrimination during photosynthesis by comparing observed values with those derived from a model-based prediction of discrimination under infinite mesophyll conductance. This approach requires a high precision in discrimination records, which is now achieved by combining precise leaf gas exchange measurements with online TDL-AS records of changes in $^{13}CO_2/^{12}CO_2$ in the atmosphere around the leaf (for a discussion of the technique, see Pons *et al*, 2009; Tazoe *et al.*, 2011). One of the important problems with this method is the fact that several discrimination steps during photosynthesis, respiration, and photorespiration need be taken into account. In particular, a number of earlier studies omitted the respiratory and photorespiratory terms (Flexas *et al.*, 2007b; Vrabl *et al.*, 2009). Moreover, the response of g_m to CO_2 was affected by the O_2 mole fraction in the air; that is, by the occurrence of photorespiration during measurements: it was visible only under low O_2 (Tazoe *et al.*, 2011).

In the present study, these two terms were incorporated into the g_m estimates displayed in the results. Absolute values of g_m were up to 50% larger when these terms were incorporated, and this enhancement was independent of the treatments applied (Fig. 6). Whether this potentially large change had an impact on the observed the effects of changing the CO_2 mole fraction in the air or irradiance was tested: the response of g_m to CO_2 mole fraction and irradiance remained significant even when the respiratory term was omitted (see Table 2). the effects of substituting e (fractionation during day respiration) and f (fractionation during photorespiration) with extreme values ($f=0‰$, $e= -10‰$, $e= +10‰$) were similarly tested. Despite the fact that these changes resulted in significant differences of computed g_m, they did not result in any loss of significance of the observed effects of CO_2 or irradiance (data not shown). Vrabl *et al.* (2009) compared g_m estimated with the fluorescence method (which takes the respiratory terms implicitly into account) and with the isotopic method (without taking them into account) and found the same

range of g_m values and the same negative response to C_i. The present computations suggest that the respiratory terms can be important in the estimation of the absolute values of g_m, but have only little influence on the observed CO_2 or irradiance responses of g_m. The respiratory terms of isotopic discrimination are unlikely to be responsible for the discrepancies among studies. Addressing the question of changing e and f during the CO_2 and irradiance treatments was omitted in this discussion: up to now there is no reason to assume that these values are not stable across the whole range of environmental conditions.

Table 2. Impact of omitting the respiratory term in the discrimination model on the assessment of the impact of the CO_2 mole fraction (C_i) or of irradiance on g$_m$

Mixed effect model for mesophyll conductance computed including (as shown in Table 1) or omitting the respiration and photorespiration terms.

		C$_i$		PPFD	
		g_m	g_m (omitting the respiration terms)	g_m	g_m (omitting the respiration terms)
Variable	F	18.67	13.14	6.41	12.09
	P	<0.001	0.001	0.002	<0.001
Species	F	10.11	10.28	NS	4.89
	P	0.006	0.006	NS	0.03
Interaction	F	3.44	3.64	NS	NS
	P	0.047	0.04	NS	NS
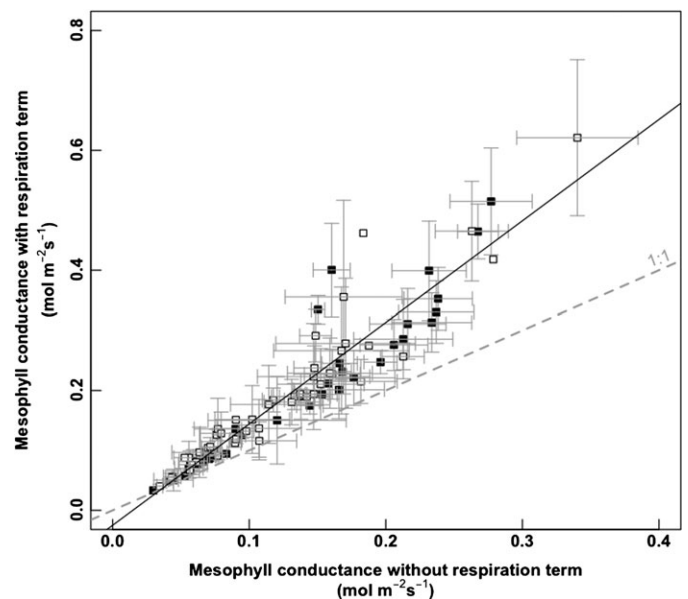
Fig. 6. Mesophyll conductance g_m as computed by taking into account the contribution of respiration and photorespiration to $^{13}CO_2$ discrimination versus without taking them into account (i.e. fractionation factors e and f set to 0 in Equation 7). Results obtained under changing CO_2 (filled squares) or irradiance (open squares). The dashed line represents the 1:1 relationship. Each point represents the mean $\pm$SE of a given measurement ($n=3$).

Response of g$_m$ to CO_2 mole fraction

There was at maximum a 50% decrease in g_m with increasing CO_2 mole fraction (from 300 μmol mol^{-1} to 900 μmol mol^{-1}). This response was general, as all three species displayed a similar response to CO_2, with the exception of a single individual of *E. sieberi*. The results contrast with earlier studies reporting no response of g_m to CO_2. This was the case in *Quercus ilex* and *Citrus aurantium* (chlorophyll fluorescence method; Loreto *et al.*, 1992), *Raphanus sativus* (isotopic discrimination; Von Caemmerer and Evans, 1991), and *Triticum aestivum* (isotopic discrimination; Tazoe *et al.*, 2009). The present results confirm several studies that reported a negative relationship between g_m and CO_2 (Flexas *et al.*, 2007b; Hassiotou *et al.*, 2009; Vrabl *et al.*, 2009; Bunce, 2010). The same magnitude of decrease of g_m with C_i as in Flexas *et al.* (2007b) and Vrabl *et al.* (2009) was found. Tazoe *et al.* (2011) found an ~30% decrease of g_m when C_i increased under 1% O_2 but no effect under 21% O_2 in two *Arabidopsis thaliana* genotypes or in *Nicotinia tabacum*, while in the present study a significant effect was found even under 21% O_2. The absence of a clear pattern of g_m responses among studies could be interpreted as a species-dependent response of g_m to C_i, but no common trait seems to be shared by the 'non-responsive' versus the 'responsive' species.

There are a suite of methodological reasons and artefacts (e.g. choice or calculation of *b*, *e*, *f*, R_d, or Γ^*) that might explain the discrepancy among studies. The case for *e* and *f* was discussed above. Measured values of R_d and Γ^* (i.e. of its proxy C_i^*) were used for each species rather than arbitrary values taken from the literature. Despite some uncertainties regarding the choice of *b* or *f* (Lanigan *et al.*, 2008; Pons *et al.*, 2009), it is concluded that the response of g_m that was recorded here is unlikely to be an artefact.

Rapid responses of g_m to CO_2 could be mediated by aquaporins that might impact the permeability of plasma and chloroplast membranes to CO_2 (Terashima and Ono, 2002), enhancing CO_2 diffusion in the liquid phase. Flexas *et al.* (2006) stated that the expression of NtAQP1 aquaporins can change g_m values by 20–50% in *N. tabacum*. These variations of g_m are of the same magnitude as those in the present study, but only direct measurements of aquaporin expression/activity could confirm the role of these proteins in the diffusion of CO_2 through membranes. Establishing a parallel between short-term responses of g_m and of the expression and activities of aquaporins is still an open area for research. Tholen *et al.* (2008) also found that chloroplast movements can induce a variation of g_m by 50% in *A. thaliana*. However, it is not known yet whether CO_2 variations can directly mediate a displacement of chloroplasts.

A positive relationship was observed between g_m and g_s, as was also observed by Flexas *et al.* (2007c). Interestingly, such a relationship was also found by Flexas *et al.* (2006) when they compared plants overexpressing NtAQP1 aquaporin and controls. They suggested that the variation of g_m primarily induced by manipulating NtAQP1 expression probably also led to an adjustment of g_s and subsequently of *A*. This potentially indicates a physiological link between these two parameters (Flexas *et al.*, 2007c; Vrabl *et al.*, 2009). Nevertheless, the precise signalling cascade that could cause a coordinated response of stomatal and of mesophyll conductance remains to be elucidated.

Response of g$_m$ to irradiance

Several studies observed an increase in g_m with increasing irradiance. Flexas *et al.* (2007b) reported that g_m increased in tobacco by ~40% when irradiance increased from 250 μmol m^{-2} s^{-1} to 1000 μmol m^{-2} s^{-1}. Data from Gorton *et al.* (2003), reanalysed by Flexas *et al.* (2008), also showed a positive effect of irradiance on g_m. Hassiotou *et al.* (2009) detected an ~22% increase in six *Banksia* species as irradiance was switched from 500 μmol m^{-2} s^{-1} to 1500 μmol m^{-2} s^{-1}. The present study corroborates this positive effect of irradiance, with an increase in g_m by 60%, up to a plateau in irradiance reached between 500 μmol m^{-2} s^{-1} and 1100 μmol m^{-2} s^{-1}, depending on the species. A slightly larger sensitivity of g_m to irradiance than earlier studies was found. Sensitivity to irradiance could be (i) species dependent or (ii) due to different parameterization of the model enabling g_m estimation. For instance, in the present case, removing the respiratory and photorespiratory terms in the estimation of g_m led to a slightly smaller response of g_m to irradiance (Table 2). A systematic analysis of the reported responses, with a standardized parameterization, would be very helpful.

As during the response to CO_2, g_m was positively correlated to g_s. This relationship seems to be independent of the method used to vary net CO_2 assimilation rates. A review by Flexas *et al.* (2008) insisted that g_s and g_m responded in parallel to irradiance, CO_2, temperature, and drought stress (Warren, 2008b). On the other hand, Warren (2008b) reported that g_m was unaffected by increases in vapour pressure deficit (VPD) while g_s decreased strongly, and Vrabl *et al.* (2009) reported that g_m was unaffected by feeding leaves with abscisic acid (ABA), whereas there was a clear decrease in g_s. In the two latter cases the net CO_2 assimilation rate remained unaffected by VPD and ABA despite the severe reduction of g_s. The g_s–g_m relationship therefore may reflect a tight coordination between *A* and g_m. Thus it seems that g_m contributes to adjust the CO_2 supply to the sites of carboxylation in response to photosynthetic limitations such as light availability, hydraulic constraints, or biochemical limitations (Warren *et al.*, 2007). In the present study, the coordinated variations of g_s and g_m apparently led to a very stable C_c (and C_i–C_c drawdown) across irradiance levels, despite large variation in *A*. Such a homeostasis of C_c was already observed across a range of leaf morphologies (Hassiotou *et al.*, 2009), during leaf ageing (Ethier *et al.*, 2006; Warren, 2006), and such an adjustment seems also to occur during short-term fluctuations of irradiance.

Conclusion

This study with three *Eucalyptus* species confirmed that g_m estimated with the online ^{13}C discrimination method declines in response to short-term increases of the CO_2 mole fraction and increases with irradiance. The response to irradiance is saturated above 500 μmol m^{-2} s^{-1} PPFD. The respiratory term in the ^{13}C discrimination equation was found to be important to estimate absolute values of g_m but had little impact on the CO_2 and irradiance responses. During the responses to CO_2 and PPFD, g_s and g_m were tightly correlated and varied in parallel independently of the source of variation. Moreover, it was observed that coordinated adjustments of CO_2 demand (A) and supply (g_s and g_m) led to a stability of C_c across irradiance variations. C_c homeostasis could be an advantage for the leaf to prevent large variation of the oxygenation/carboxylation ratio of the RubisCO, when the CO_2 demand increases.

Acknowledgements

Appendix I

Here we describe the procedure to calculate the standard deviation of Δ_{obs} ($Sd_{\Delta obs}$) based on the standard deviation of the isotopic composition of reference and measured air ($Sd_{\delta 13Ce}$ and $Sd_{\delta 13Co}$, respectively). In the equation of Evans *et al.* (1986) to calculate Δ_{obs}, $\delta^{13}C_e$ and $\delta^{13}C_o$ were substituted by their respective standard errors $Sd_{\delta 13Ce}$ and $Sd_{\delta 13Co}$ to obtain:

$$Sd_{\Delta obs} \approx \frac{\xi(Sd_{\delta 13Co} - Sd_{\delta 13Ce})}{1 + Sd_{\delta 13Co} - \xi(Sd_{\delta 13Co} - Sd_{\delta 13Ce})}$$

$(Sd_{\delta 13Co} - Sd_{\delta 13Ce})$ and $Sd_{\delta 13Co}$ were replaced by $\sqrt{Sd_{\delta 13Co}^2 + Sd_{\delta 13Ce}^2}$ and $\sqrt{Sd_{\delta 13Co}^2}$, respectively, as is described in Harris (1991) to obtain:

$$Sd_{\Delta obs} \approx \frac{\xi\sqrt{Sd_{\delta 13Co}^2 + Sd_{\delta 13Ce}^2}}{1 + \sqrt{Sd_{\delta 13Co}^2} - \xi\sqrt{Sd_{\delta 13Co}^2 + Sd_{\delta 13Ce}^2}}$$

Then, to calculate the cumulative effect of the upper term and the lower term, their relative Sds were summed to obtain the relative standard error of Δ_{obs}:

$$\frac{Sd_{\Delta obs}}{\Delta_{obs}} = \left(\frac{\xi\sqrt{Sd_{\delta 13Co}^2 + Sd_{\delta 13Ce}^2}}{\xi(\delta^{13}C_o - \delta^{13}C_e)}\right)$$
$$+ \left(\frac{1 + \sqrt{Sd_{\delta 13Co}^2} - \xi\sqrt{Sd_{\delta 13Co}^2 + Sd_{\delta 13Ce}^2}}{1 + \delta^{13}C_o - \xi(\delta^{13}C_o - \delta^{13}C_e)}\right)$$

$Sd_{\Delta obs}$ is then equal to:

$$Sd_{\Delta obs} = \left(\frac{\xi\sqrt{Sd_{\delta 13Ce}^2 + Sd_{\delta 13Co}^2}}{\xi(\delta^{13}C_o - \delta^{13}C_e)}\right.$$
$$\left. + \frac{1 + \sqrt{Sd_{\delta 13Co}^2} - \xi\sqrt{Sd_{\delta 13Ce}^2 + Sd_{\delta 13Co}^2}}{1 + \delta^{13}C_o - \xi(\delta^{13}C_o - \delta^{13}C_e)}\right)\Delta_{obs}$$

References

Ball JT. 1987. Calculations related to gas exchange. In: Zeiger EF, Farquhar GD, Cowan IR, eds. *Stomatal function*. Stanford, CA: Stanford University Press, 445–476.

Bernacchi CJ, Portis AR, Nakano H, Von Caemmerer S, Long SP. 2002. Temperature response of mesophyll conductance. *Implications for the determination of Rubisco enzyme kinetics and for limitations to photosynthesis in vivo. Plant Physiology* **130,** 1992–1998.

Bongi G, Loreto F. 1989. Gas-exchange properties of salt-stressed olive (*Olea europea* L.) leaves. *Plant Physiology* **90,** 1408–1416.

Brooks A, Farquhar GD. 1985. Effect of temperature on the CO_2/O_2 specificity of ribulose-1,5-bisphosphate carboxylase oxygenase and the rate of respiration in the light—estimates from gas-exchange measurements on spinach. *Planta* **165,** 397–406.

Bunce J. 2010. Variable responses of mesophyll conductance to substomatal carbon dioxide concentration in common bean and soybean. *Photosynthetica* **48,** 507–512.

Cornic G, Legouallec JL, Briantais JM, Hodges M. 1989. Effect of dehydration and high light on photosynthesis of 2 C_3 plants (*Phaseolus vulgaris* L. and *Elatostema repens* (Lour) Hall F). *Planta* **177,** 84–90.

During H. 2003. Stomatal and mesophyll conductances control CO_2 transfer to chloroplasts in leaves of grapevine (*Vitis vinifera* L.). *Vitis* **42,** 65–68.

Epron D, Godard D, Cornic G, Genty B. 1995. Limitation of net CO_2 assimilation rate by internal resistances to CO_2 transfer in the leaves of 2 tree species (*Fagus sylvatica* L. and *Castanea sativa* Mill). *Plant, Cell and Environment* **18,** 43–51.

Ethier GJ, Livingston NJ, Harrison DL, Black TA, Moran JA. 2006. Low stomatal and internal conductance to CO_2 versus Rubisco

deactivation as determinants of the photosynthetic decline of ageing evergreen leaves. *Plant, Cell and Environment* **29,** 2168–2184.

Evans JR, Kaldenhoff R, Genty B, Terashima I. 2009. Resistances along the CO_2 diffusion pathway inside leaves. *Journal of Experimental Botany* **60,** 2235–2248.

Evans JR, Sharkey TD, Berry JA, Farquhar GD. 1986. Carbon isotope discrimination measured concurrently with gas-exchange to investigate CO_2 diffusion in leaves of higher-plants. *Australian Journal of Plant Physiology* **13,** 281–292.

Evans JR, Von Caemmerer S. 1996. Carbon dioxide diffusion inside leaves. *Plant Physiology* **110,** 339–346.

Farquhar GD, O'Leary MH, Berry JA. 1982. On the relationship between carbon isotope discrimination and the inter-cellular carbon-dioxide concentration in leaves. *Australian Journal of Plant Physiology* **9,** 121–137.

Farquhar GD, Richards RA. 1984. Isotopic composition of plant carbon correlates with water-use efficiency of wheat genotypes. *Australian Journal of Plant Physiology* **11,** 539–552.

Farquhar GD, Von Caemmerer S, Berry JA. 1980. A biochemical-model of photosynthetic CO_2 assimilation in leaves of C_3 species. *Planta* **149,** 78–90.

Flexas J, Diaz-Espejo A, Berry JA, Cifre J, Galmes J, Kaldenhoff R, Medrano H, Ribas-Carbo M. 2007. *a.* Analysis of leakage in IRGA's leaf chambers of open gas exchange systems: quantification and its effects in photosynthesis parameterization. *Journal of Experimental Botany* **58,** 1533–1543.

Flexas J, Diaz-Espejo A, Galmes J, Kaldenhoff R, Medrano H, Ribas-Carbo M. 2007. *b.* Rapid variations of mesophyll conductance in response to changes in CO_2 concentration around leaves. *Plant, Cell and Environment* **30,** 1284–1298.

Flexas J, Ortuno MF, Ribas-Carbo M, Diaz-Espejo A, Florez-Sarasa ID, Medrano H. 2007 *c.* Mesophyll conductance to CO_2 in. *Arabidopsis thaliana. New Phytologist* **175,** 501–511.

Flexas J, Ribas-Carbo M, Diaz-Espejo A, Galmes J, Medrano H. 2008. Mesophyll conductance to CO_2: current knowledge and future prospects. *Plant, Cell and Environment* **31,** 602–621.

Flexas J, Ribas-Carbo M, Hanson DT, Bota J, Otto B, Cifre J, McDowell N, Medrano H, Kaldenhoff R. 2006. Tobacco aquaporin NtAQP1 is involved in mesophyll conductance to CO_2 *in vivo*. *The Plant Journal* **48,** 427–439.

Gaastra P. 1959. Photosynthesis of crop plants as influenced by light, carbon dioxide, temperature and stomatal diffusion resistance. *Mededelingen van de Landbouhoogeschool te Wageningen* **59,** 1–68.

Ghashghaie J, Badeck F, Lanigan GJ, Nogues S, Tcherkez G, Deleens E, Cornic G, Griffiths H. 2003. Carbon isotope fractionation during dark respiration and photorespiration in C_3 plants. *Phytochemistry Reviews* **2,** 145–61.

Gorton HL, Herbert SK, Vogelmann TC. 2003. Photoacoustic analysis indicates that chloroplast movement does not alter liquid-phase CO_2 diffusion in leaves of *Alocasia brisbanensis. Plant Physiology* **132,** 1529–1539.

Harley PC, Loreto F, Dimarco G, Sharkey TD. 1992. Theoretical considerations when estimating the mesophyll conductance to CO_2 flux by analysis of the response of photosynthesis to CO_2. *Plant Physiology* **98,** 1429–1436.

Harris DC. 1991. *Quantitative chemical analysis*. New York: WH Freeman and Company.

Hassiotou F, Ludwig M, Renton M, Veneklaas EJ, Evans JR. 2009. Influence of leaf dry mass per area, CO_2, and irradiance on mesophyll conductance in sclerophylls *Journal of Experimental Botany* **60,** 2303–2314.

Lanigan GJ, Betson N, Griffiths H, Seibt U. 2008. Carbon isotope fractionation during photorespiration and carboxylation in senecio. *Plant Physiology* **148,** 2013–20.

Lloyd J, Syvertsen JP, Kriedemann PE, Farquhar GD. 1992. Low conductances for CO_2 diffusion from stomata to the sites of carboxylation in leaves of woody species. *Plant, Cell and Environment* **15,** 873–899.

Loreto F, Harley PC, Dimarco G, Sharkey TD. 1992. Estimation of mesophyll conductance to CO_2 flux by 3 different methods. *Plant Physiology* **98,** 1437–1443.

Niinemets U, Diaz-Espejo A, Flexas J, Galmes J, Warren CR. 2009*a.* Importance of mesophyll diffusion conductance in estimation of plant photosynthesis in the field. *Journal of Experimental Botany* **60,** 2271–2282.

Niinemets U, Diaz-Espejo A, Flexas J, Galmes J, Warren CR. 2009*b.* Role of mesophyll diffusion conductance in constraining potential photosynthetic productivity in the field. *Journal of Experimental Botany* **60,** 2249–2270.

O'Leary MH. 1981. Carbon isotope fractionation in plants. *Phytochemistry* **20,** 553–567.

Piel C, Frak E, Le Roux X, Genty B. 2002. Effect of local irradiance on CO_2 transfer conductance of mesophyll in walnut. *Journal of Experimental Botany* **53,** 2423–2430.

Pons TL, Flexas J, von Caemmerer S, Evans JR, Genty B, Ribas-Carbo M, Brugnoli E. 2009. Estimating mesophyll conductance to CO_2: methodology, potential errors, and recommendations. *Journal of Experimental Botany* **60,** 2217–2234.

Pons TL, Welschen RAM. 2003. Midday depression of net photosynthesis in the tropical rainforest tree *Eperua grandiflora*: contributions of stomatal and internal conductances, respiration and Rubisco functioning. *Tree Physiology* **23,** 937–947.

Rodeghiero M, Niinemets Ü Cescatti A. 2007. Major diffusion leaks of clamp-on leaf cuvettes still unaccounted: how erroneous are the estimates of Farquhar *et al*. model parameters? *Plant, Cell and Environment* **30,** 1006–1022.

Roupsard O, Gross P, Dreyer E. 1996. Limitation of photosynthetic activity by CO_2 availability in the chloroplasts of oak leaves from different species and during drought. *Annales des Sciences Forestières* **53,** 243–254.

Scartazza A, Lauteri M, Guido MC, Brugnoli E. 1998. Carbon isotope discrimination in leaf and stem sugars, water-use efficiency and mesophyll conductance during different developmental stages in rice subjected to drought. *Australian Journal of Plant Physiology* **25,** 489–498.

Tazoe Y, Von Caemmerer S, Badger MR, Evans JR. 2009. Light and CO_2 do not affect the mesophyll conductance to CO_2 diffusion in wheat leaves. *Journal of Experimental Botany* **60,** 2291–2301.

Tazoe Y, Von Caemmerer S, Estavillo GM, Evans JR. 2011. Using tunable diode laser spectroscopy to measure carbon isotope discrimination and mesophyll conductance to CO_2 diffusion dynamically at different CO_2 concentrations. *Plant, Cell and Environment* **34,** 580–591.

Tcherkez G. 2006. How large is the carbon isotope fractionation of the photorespiratory enzyme glycine decarboxylase? *Functional Plant Biology* **33,** 911–920.

Terashima I, Hanba YT, Tazoe Y, Vyas P, Yano S. 2006. Irradiance and phenotype: comparative eco-development of sun and shade leaves in relation to photosynthetic CO_2 diffusion. *Journal of Experimental Botany* **57,** 343–354.

Terashima I, Ono K. 2002. Effects of $HgCl_2$ on CO_2 dependence of leaf photosynthesis: evidence indicating involvement of aquaporins in CO_2 diffusion across the plasma membrane. *Plant and Cell Physiology* **43,** 70–78.

Tholen D, Boom C, Noguchi K, Ueda S, Katase T, Terashima I. 2008. The chloroplast avoidance response decreases internal conductance to CO_2 diffusion in *Arabidopsis thaliana* leaves. *Plant, Cell and Environment* **31,** 1688–1700.

Viil J, Laisk A, Oja V, Parnik T. 1977. Enhancement of photosynthesis caused by oxygen under saturating irradiance and high CO_2 concentrations. *Photosynthetica* **11,** 251–259.

Von Caemmerer S, Evans JR. 1991. Determination of the average partial-pressure of CO_2 in chloroplasts from leaves of several C_3 plants. *Australian Journal of Plant Physiology* **18,** 287–305.

Von Caemmerer S, Evans JR, Hudson GS, Andrews TJ. 1994. The kinetics of ribulose-l,5-bisphosphate carboxylase/oxygenase *in vivo* inferred from measurements of photosynthesis in leaves of transgenic tobacco. *Planta* **195,** 88–97.

Vrabl D, Vaskova M, Hronkova M, Flexas J, Santrucek J. 2009. Mesophyll conductance to CO_2 transport estimated by two independent methods: effect of variable CO_2 concentration and abscisic acid. *Journal of Experimental Botany* **60,** 2315–2323.

Warren CR. 2006. Why does photosynthesis decrease with needle age in *Pinus pinaster? Trees-Structure and Function* **20,** 157–164.

Warren CR. 2008a. Does growth temperature affect the temperature responses of photosynthesis and internal conductance to CO_2? A test with. *Eucalyptus regnans. Tree Physiology* **28,** 11–19.

Warren CR. 2008b. Soil water deficits decrease the internal conductance to CO_2 transfer but atmospheric water deficits do not. *Journal of Experimental Botany* **59,** 327–334.

Warren CR, Adams MA. 2006. Internal conductance does not scale with photosynthetic capacity: implications for carbon isotope discrimination and the economics of water and nitrogen use in photosynthesis. *Plant, Cell and Environment* **29,** 192–201.

Warren CR, Dreyer E. 2006. Temperature response of photosynthesis and internal conductance to CO_2: results from two independent approaches. *Journal of Experimental Botany* **57,** 3057–3067.

Warren CR, Low M, Matyssek R, Tausz M. 2007. Internal conductance to CO_2 transfer of adult *Fagus sylvatica*: variation between sun and shade leaves and due to free-air ozone fumigation. *Environmental and Experimental Botany* **59,** 130–138.

Wingate L, Seibt U, Moncrieff JB, Jarvis PG, Lloyd J. 2007. Variations in ^{13}C discrimination during CO_2 exchange by *Picea sitchensis* branches in the field. *Plant, Cell and Environment* **30,** 600–616.

Yamori W, Evans JR, Von Caemmerer S. 2010. Effects of growth and measurement light intensities on temperature dependence of CO_2 assimilation rate in tobacco leaves. *Plant, Cell and Environment* **33,** 332–343.